Comparison of Respiratory Motion Suppression Techniques for 4D Flow MRI

Petter Dyverfeldt[1,2]* and Tino Ebbers[1,2]

Purpose: The purpose of this work was to assess the impact of respiratory motion and to compare methods for suppression of respiratory motion artifacts in 4D Flow MRI.
Methods: A numerical 3D aorta phantom was designed based on an aorta velocity field obtained by computational fluid mechanics. Motion-distorted 4D Flow MRI measurements were simulated and several different motion-suppression techniques were evaluated: Gating with fixed acceptance window size, gating with different window sizes in inner and outer k-space, and k-space reordering. Additionally, different spatial resolutions were simulated.
Results: Respiratory motion reduced the image quality. All motion-suppression techniques improved the data quality. Flow rate errors of up to 30% without gating could be reduced to less than 2.5% with the most successful motion suppression methods. Weighted gating and gating combined with k-space reordering were advantageous compared with conventional fixed-window gating. Spatial resolutions finer than the amount of accepted motion did not lead to improved results.
Conclusion: Respiratory motion affects 4D Flow MRI data. Several different motion suppression techniques exist that are capable of reducing the errors associated with respiratory motion. Spatial resolutions finer than the degree of accepted respiratory motion do not result in improved data quality.

Key words: motion suppression; 4D flow MRI; MR flow imaging; artifacts; image quality; navigator gating

INTRODUCTION

Noncompensated respiratory motion causes ghosting and blurring artifacts in MRI and several approaches to suppress the effects of respiratory motion have been proposed (1–12). For scans longer than 15–20 s, the most commonly used approach is that of navigator gating, sometimes combined with a respiratory-based k-space reordering scheme. Respiratory gating is typically achieved by using a pencil-beam or cross-pair excitation to acquire a column of pixels across the lung-to-liver interface track the position of the diaphragm. Recently, conventional navigators have been complemented by a variety of self-gating methods.

By only accepting data acquired when the tracked structure is near the end-expiratory position, the use of gating typically results in increased scan time. Especially for applications with long nominal scan time, the additional scan time imposed by the gating efficiency can be lengthy and thus increase the discomfort of the patient as well as the cost of the scan. One such application is 4D Flow MRI, where nominal scan times of around 10 min result in excessively long scan times of around 20 min when the gating efficiency is around 50%.

The impact of different options for suppression of respiratory motion in 4D Flow MRI has not been evaluated in detail. This may partly be due to the wide variety of applications of 4D Flow MRI, which makes standardization challenging (13). In coronary MRI, where measures such as lumen-to-wall sharpness and lumen-to-wall contrast-to-noise ratio are relevant and easily accessible quantitative measures of image quality, the effects of respiratory motion on image quality have been studied in more detail and this has led to new developments within respiratory motion suppression (5,6,8,10–12,14). For 4D Flow MRI, on the other hand, the trend seems to go towards less respiratory suppression.

While several different approaches have been explored to reduce the scan time penalty imposed by respiratory gating in 4D Flow MRI (7,15–18), recent 4D Flow MRI studies have suggested that 4D Flow MRI-based aorta flow volume quantification does not require respiratory motion suppression (19,20). Another recent study suggested not taking respiratory effects in cardiac 4D Flow MRI into account at all (21). However, to neglect respiratory motion without reducing the spatial resolution according to the expected range of motion seems counterintuitive as the effect of global motion on an MR image can be represented by a degradation of spatial resolution corresponding to convolution between a motion-free image and the position-distribution function of the motion (3).

The aim of this study was, therefore, to assess the effects of respiratory motion suppression techniques methods commonly used in 4D Flow MRI, as well as the relationship between nonsuppressed motion and reduced spatial resolution.

METHODS

Synthetic Phantom and Simulated Respiratory Motion

A simulation approach was used to assess the effects of respiratory motion and several different motion suppression

[1]Division of Cardiovascular Medicine, Department of Medical and Health Sciences, Linköping University, Linköping, Sweden.
[2]Center for Medical Image Science and Visualization (CMIV), Linköping University, Linköping, Sweden.
Grant sponsor: the European Research Council; Grant numbers: HEART4-FLOW, 310612; Grant sponsor: Swedish Research Council.
*Correspondence to: Petter Dyverfeldt, Ph.D., Division of Cardiovascular Medicine, Department of Medical and Health Sciences, Linköping University, SE-58183 Linköping, Sweden. E-mail: petter.dyverfeldt@liu.se
Received 3 October 2016; revised 11 November 2016; accepted 17 November 2016
DOI 10.1002/mrm.26574
Published online 11 January 2017 in Wiley Online Library (wileyonlinelibrary.com).

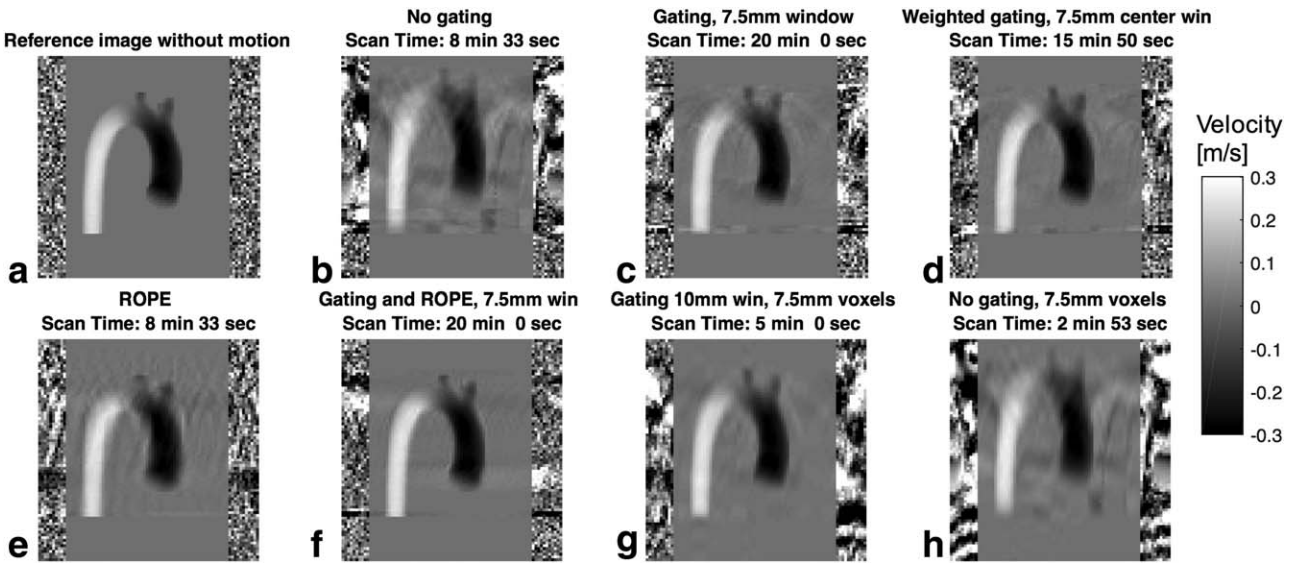

FIG. 1. Mean intensity projections of velocity images for reference image without motion (**A**), no gating (**B**), gating with 10 mm window (**C**), weighted gating with 10 mm inner window no outer window (**D**), ROPE (**E**), gating with 10 mm window combined with ROPE (**F**), gating with 10 mm window and voxel size reduced to 10 mm in feet-to-head direction (**G**), and no gating and voxel size reduced to 10 mm in feet-to-head direction (**H**).

techniques. A synthetic 3D aorta phantom was constructed from a peak-systolic 3D numerical velocity data set of an aorta. The numerical velocity data was obtained as described in Lantz et al. (22). Stationary tissue, simulating the thorax, was added around the aorta. The stationary tissue and the aorta were assigned signal amplitudes of 100 and 200 (a.u.), respectively. Respiratory motion was simulated by subjecting the synthetic phantom to a sinusoidal motion pattern in the feet-to-head direction. For simplicity, the object was considered rigid and thus the whole object underwent the same motion. The frequency of the sinusoidal motion was 12 breaths per min and the maximum amplitude of motion was 24 mm, which represents a typical maximum inferior-to-superior displacement of the proximal aorta and heart due to respiratory motion (23).

MRI

Cartesian 4D Flow MRI was simulated by sampling k-space lines at 1-s time intervals, corresponding to 4D Flow MRI without k-space segmentation at a heart rate of 60 beats per min. In this way, each k-space line corresponded to a different respiratory phase. Linear k-space view-ordering was used unless otherwise noted. The following parameters were used for all experiments: matrix size $= 80 \times 80 \times 35$, voxel size $= 2.5 \times 2.5 \times 2.5\ \text{mm}^3$, VENC $= 1.5$ m/s. For simplicity, only one time-frame was simulated.

The following respiratory motion suppression techniques were evaluated: (i) No gating. (ii) Gating with fixed window size throughout k-space. Gating window sizes of 2.5, 7.5, 12.5, 17.5, and 22.5 mm were used. (iii) Dual-window weighted gating, with smaller acceptance window for the center of k-space. This approach is available as a research option for 4D Flow MRI and other applications on Philips scanners, and was recently evaluated by Akçakaya et al. (17). Two different scenarios were included. First, the inner 50% of k-space were acquired with gating window sizes of 2.5, 7.5, 12.5, 17.5, and 22.5 mm. The window size for the outer 50% of k-space was set to three times the inner gating window. Note that this effectively suggests no outer gating for the last four cases. In the second scenario, only 9% of the inner k-space used the inner gating window. (iv) Respiratory ordered phase-encoding (ROPE) as proposed by Bailes et al. (1) and implemented for 4D Flow MRI by Markl et al. (15). (v) Gating with fixed window size throughout k-space combined with ROPE, as suggested by Wang et al. (3) and implemented for 4D Flow MRI by Markl et al. (16). Gating window sizes of 2.5, 7.5, 12.5, 17.5, and 22.5 mm were used.

As there was no drift in the end-expiratory position in the present study, the gating window was positioned with the upper limit just at the end-expiratory position. One effect of respiratory motion is that the object becomes displaced relative to its reference position, which typically is the end-expiratory position. In the present study, this displacement effect was considered secondary and we, therefore, used intensity-based rigid registration between the image and the reference object to obtain spatial alignment.

Additional experiments addressing the relationship between motion suppression and spatial resolution were carried out by simulating image acquisitions with the different motion suppression techniques for feet-to-head voxel sizes of 2.5, 5, 10, 15, 20, and 25 mm. The voxel size was not changed in the other two dimensions. All data were interpolated to 2.5 mm by using k-space zero-filling, so as to facilitate voxel-to-voxel comparisons between the different datasets.

Data Evaluation

The effect of the different motion suppression techniques on image quality was quantified by measuring the root

mean square error (RMSE) of the magnitude, velocity, and velocity gradient field. The velocity gradient field was obtained by taking the forward difference spatial derivative of the velocity field. Additionally, the percentage error in flow rate and peak velocity was measured for each motion suppression method. The flow rate was measured in the mid tubular portion of the ascending aorta, the top of the aortic arch, and the mid descending aorta.

RESULTS

The data exhibited realistic motion artifacts with blurring in the direction of motion and view-to-view artifacts with typical ghosts in the phase and slice encoding directions (Fig. 1). Visually, all motion suppression techniques resulted in improved image quality, as exemplified in Figure 1.

The effect of different motion suppression techniques on scan time and the RMSE of magnitude and velocity data is shown in Figure 2. In all cases with gating, shorter scan time is associated with larger RMSE. When compared with conventional fixed-window gating without reordering, weighted gating and gating combined with ROPE are more efficient with respect to error reduction and scan time. For example, the velocity RMSE for a scan time of 14.7 min was 24% higher for conventional fixed-window gating than weighted gating and gating combined with ROPE.

Peak velocity and flow rate estimates were affected by motion and the use of motion suppression (Fig. 3). Flow rate errors of up to 30% were detected. These errors could be reduced to less than 2.5% with the most successful gating methods. Similarly, the percentage error in peak velocity decreased from 8% for no gating to 2% when gating was successful. In general, the presence of motion led to underestimation of peak velocity and the use of motion suppression reduced the underestimation. Similarly, larger degrees of nonsuppressed motion led to flow rate estimates that deviated more from the true value. The improvements in flow parameter estimation with longer scan time was more pronounced for gating and weighted gating than for gating combined with ROPE, because ROPE helps to reduce errors also with a large gating window. For example, an increase in scan time from 9 to 15 min lead to an improvement in the ascending aorta flow rate estimation of 26 mL/s, or 5%, for gating and 7 mL/s, or 1%, for gating combined with ROPE.

The relationship between spatial resolution, respiratory motion suppression and image quality is explored in Figure 4. For the case without motion, or when the voxel size is sufficiently large relative to the amount of nonsuppressed motion, the RMSE is reduced when the spatial resolution is improved. However, smaller voxel size does not reduce the RMSE when the voxel size is small relative to the gating window size. This is seen most clearly for the fixed-window gating results. Also, the upsampling of spatial resolution by k-space zero filling to 2.5 mm for all acquired voxel sizes resulted in a smoothing effect that reduced the velocity RMSE and especially the velocity gradient RMSE for voxel sizes that were small relative to the amount of nonsuppressed motion (see Figure 4). For example, this is seen in the velocity gradient RMSE results for the case of 17.5 mm gating window with 10, 5, and 2.5 mm voxel sizes in Figure 4C. Similar effects are seen in Figure 3 where an increase in spatial resolution from 5 mm to 2.5 mm does not improve the peak velocity or flow rate estimation for fixed-window gating with 7.5 mm gating window (cyan line in Figure 3).

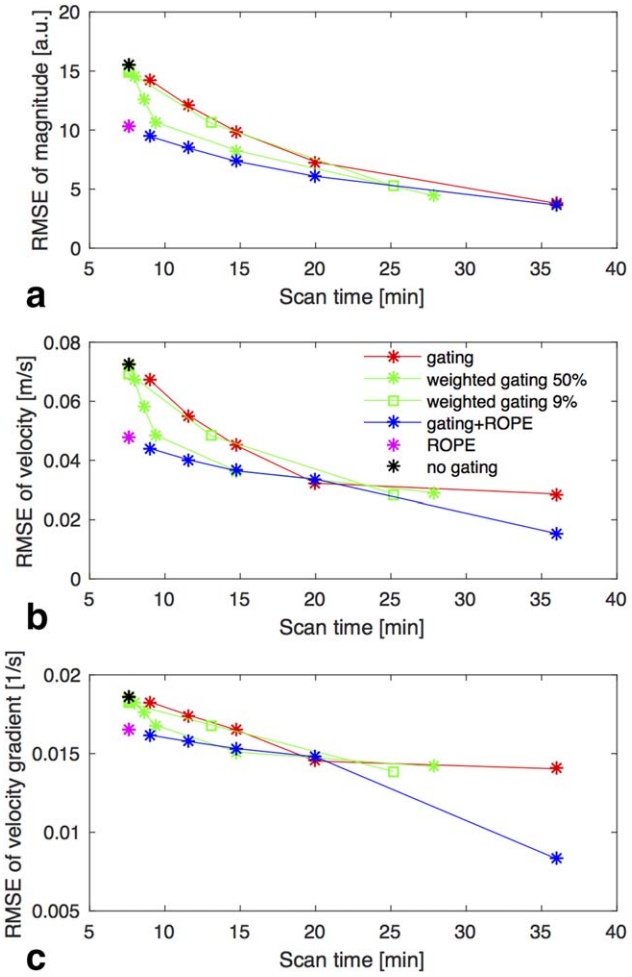

FIG. 2. Root mean square error (RMSE) versus scan time for magnitude (**A**) and velocity (**B**), and velocity gradient (**C**) data relative to the reference image without motion. Different scan times were obtained by using different motion suppression techniques and gating window sizes; tighter windows are associated with the longer scan times. Red line: Conventional fixed-window gating for gating windows of 2.2.5, 7.5, 12.5, 17.5, and 22.5. Green line with asterisks: Weighted gating for gating windows of 2.5, 7.5, 12.5, 17.5, and 22.5 in the inner 50% of k-space and 3 × the inner gate in the outer 50% of k-space. Green line with squares: Weighted gating for gating windows of 2.5, 7.5, 12.5, 17.5, and 22.5 in the inner 9% of k-space and 3 × the inner gate in the outer 91% of k-space. Blue line: Fixed-window gating combined with k-space-reordering method ROPE for gating windows of 2.5, 7.5, 12.5, 17.5, and 22.5. Magenta asterisk: ROPE. Black asterisk: No gating.

DISCUSSION

Several different approaches to suppress the effects of respiratory motion in 4D Flow MRI were evaluated. As

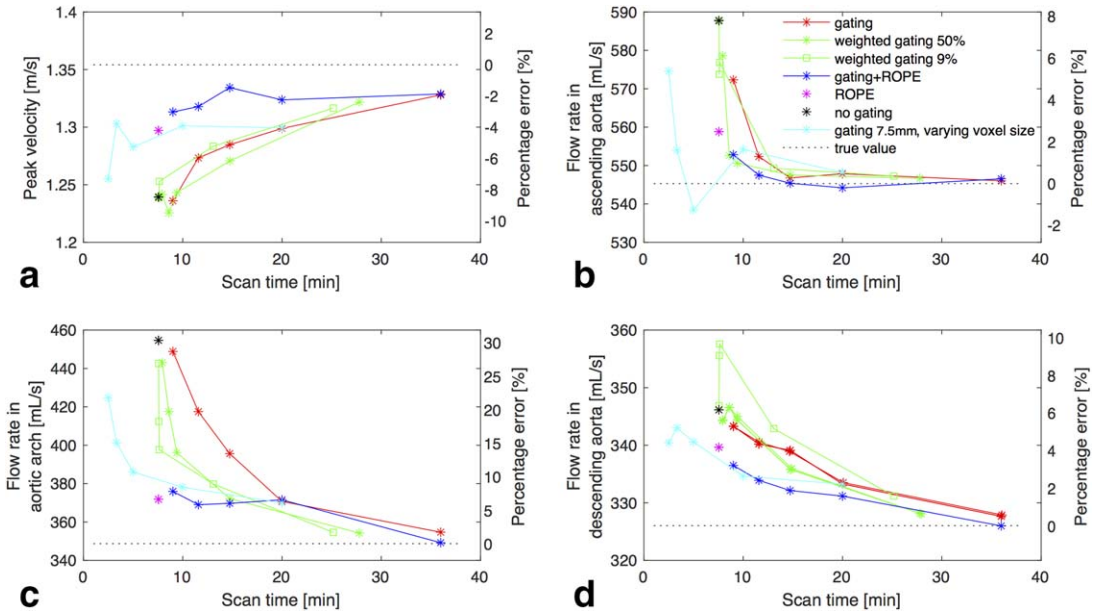

FIG. 3. Aorta peak velocity (**A**) and flow rate estimates in the ascending aorta (**B**), aortic arch (**C**) and descending aorta (**D**) plotted versus scan time. Different scan times were obtained by using different motion-suppression techniques and gating thresholds or voxel sizes. Red line: Conventional fixed-window gating for gating windows of 2.5, 7.5, 12.5, 17.5, and 22.5. Green line with asterisks: Weighted gating for gating windows of 2.5, 7.5, 12.5, 17.5, and 22.5 in the inner 50% of k-space and 3 × the inner gate in the outer 50% of k-space. Green line with squares: Weighted gating for gating windows of 2.5, 7.5, 12.5, 17.5, and 22.5 in the inner 9% of k-space and 3 × the inner gate in the outer 91% of k-space. Dark blue line: Fixed-window gating combined with k-space-reordering method ROPE for gating windows of 2.5, 7.5, 12.5, 17.5, and 22.5. Magenta asterisk: ROPE. Black asterisk: No gating. Light blue line: Fixed-window gating with 10-mm gating window and feet-to-head voxel sizes of 2.5, 5, 10, 15, and 20 mm.

with other studies, we found that respiratory motion degrades image quality and that motion suppression techniques can effectively reduce the degradation of image quality.

The RMSE of the measured velocity field as well as the velocity gradient field, flow rate, and peak velocity were all affected by respiratory motion. Motion distorts MR images in two primary ways: view-to-view ghosts and blurring. While the impact of ghosting on quantitative flow parameters can be difficult to predict, blurring corresponds to convolution between a motion-free image and the position-distribution function of the motion (3).

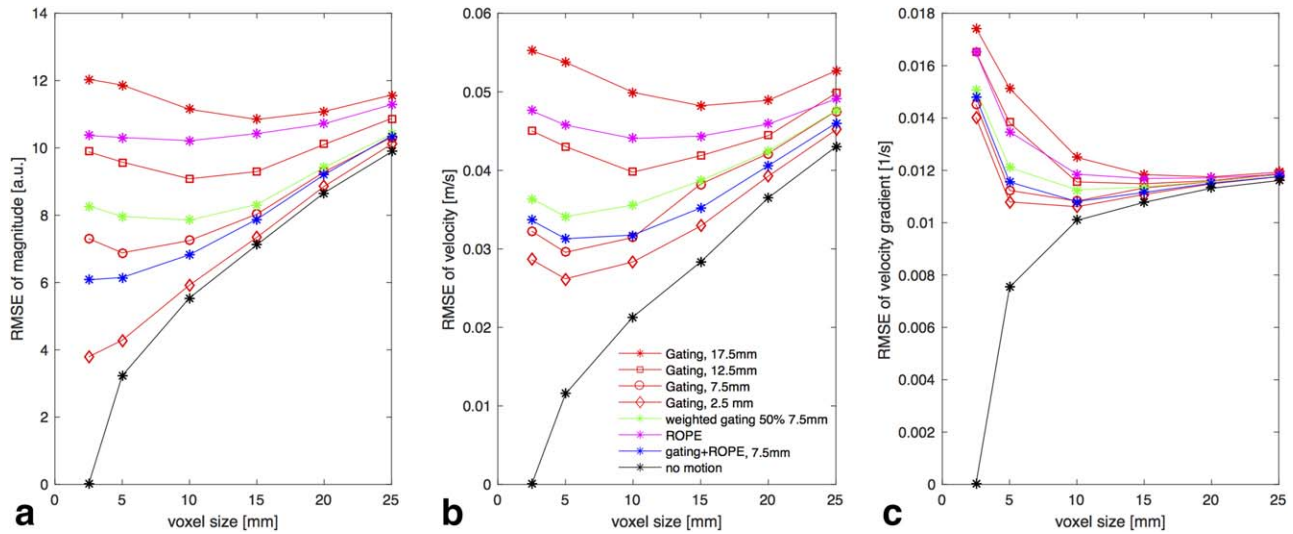

FIG. 4. Effect of spatial resolution on root mean square error (RMSE) of magnitude (**A**), velocity (**B**), and velocity gradient (**C**) data relative to the reference image without motion for different motion suppression methods. The horizontal axis denotes voxel size in the feet-to-head direction. Red lines: Conventional fixed-window gating for gating windows of 5 (diamonds), 10 (circles), 15 (squares), and 20 (asterisks). Green line: Weighted gating for gating windows of 10 mm the inner 50% of k-space and 30 mm in the outer 50% of k-space. Magenta line: ROPE. Dark blue line: Fixed-window gating with 10 mm window combined with k-space-reordering method ROPE. Black line: No motion.

Consequently, motion in the feet-to-head direction reduces the effective spatial resolution in this direction. As expected, our results show that increased spatial resolution does not improve image quality when the voxel size is small compared with the range of nonsuppressed motion. In agreement with theory, this suggests that the spatial resolution should be adapted to the gating window size when using conventional navigator gating, and similarly to the effectiveness of other motion suppression techniques (3).

Others have indicated that 4D Flow MRI-based quantification of flow volumes (19–21), intracardiac pathlines visualization (21), and total kinetic energy in the left atrium (21) can be performed without respiratory motion suppression. Unfortunately, the Kanski study included only eight subjects and thus the lack of significant differences between gated and nongated data may be due to underpowered statistics. Valverde et al. compared their nongated 4D Flow data against nongated 2D flow MRI with two signal averages which is insufficient to average out respiratory effects. Another study that similarly found nonsignificant differences between nongated 4D Flow and 2D flow MRI with three signal averages noted that flow volume measurements based on nonrespiratory gated 4D Flow MRI have higher variability and, therefore, inferior image quality (7).

Nevertheless, if higher variability can be accepted, the reduced image quality may under some circumstances be sufficient for estimation of robust hemodynamic parameters such as net flow. In these cases, the acquired voxel size of the 4D flow MRI acquisition should not be smaller than the degree of respiratory motion for optimal scan efficiency. The relationship between voxel size and nonsuppressed motion is highly relevant also for sequence development aimed at improved spatial resolution; improvements in spatial resolution must be combined with corresponding improvements in respiratory motion suppression.

In the present study, flow rate estimates were less affected by motion in the ascending and descending aorta, which were parallel to the direction of respiratory motion, than in the aortic arch, which was perpendicular to the direction of motion. These findings can be understood based on the fact that nonsuppressed motion corresponds to reduced effective spatial resolution. The ascending and descending aorta flow values are in practice obtained with a lower through-plane resolution, which is known to work well for 2D flow MRI. The flow values in the aortic arch, on the other hand, are obtained with a lower in-plane resolution in the feet-to-head direction and this results in severe partial volume averaging across the flow profile and with stationary tissue outside of the aorta. Future studies that assess the impact of nonsuppressed respiratory motion should, therefore, investigate different spatial resolutions, as well as flows, or flow features such as jets, in different orientations relative to the direction of motion.

As the majority of biological samples have local spectral density that is concentrated to the center of k-space, several motion suppression techniques are designed to minimize motion when this portion of the data is acquired. This is taken into account by motion-suppression methods that reorder the k-space trajectory based on the respiratory cycle, with the aim of acquiring the center of k-space during the most end-expiratory positions (1,8,10,11). This class of motion-suppression methods, commonly referred to as motion compensation methods, can also be combined with gating. A similar approach is weighted gating, which uses two or more gating windows and allows less motion for the central part of k-space. Akçakaya et al. investigated weighted gating with one 7-mm gating window for the central 4% of k-space and no gating for the outer part of k-space, and found that this provided similar 2D PC-MRI flow volume measurements as gating with a 7-mm window throughout k-space (17). Similarly, we observed only small differences between weighted gating with 50% central k-space and weighted gating with 9% central k-space. In general, we found that weighted gating and gating combined with k-space reordering were more efficient than gating with a fixed window size throughout k-space.

The simulations in this study did not include other artifacts that affect 4D Flow MRI, such as noise, eddy currents, or concomitant gradient fields. Eddy currents and concomitant gradient fields introduce phase offsets that are independent of respiratory motion artifacts. Typical noise levels are not expected to affect the assessment of flow rate measurements, but would affect RMSE measurements. With the simulation approach used here, motion-related blurring artifacts would effectively smooth out noise and thus the interpretation of RMSE comparisons would be ambiguous. The use of noise-free simulations allowed us to isolate the effects of motion on the MR image and make direct RMSE comparisons between reference images and motion-distorted images.

Limitations

This study has several limitations. The synthetic phantom is a simplification of the thorax and lacks many of the structures seen in vivo. However, the aortic velocity field used here is realistic and allowed us to determine the impact of motion suppression on representative flow rate and peak velocity estimates in normal aortic flow. Peak velocity can be expected to be more affected by nonsuppressed motion in patients with localized flow jets, such as in patients with heart valve disease. While more structures could be added to the model this is not expected to alter the conclusions of the study. Another limitation is that motion was simulated only in the inferior–superior direction and the same motion was applied to the whole phantom.

Real-life in vivo respiratory motion is more complex. The degrees of error observed here should, therefore, be considered relative rather than absolute. The use of RMSE comparisons between the reference object and the motion-distorted datasets is hampered by the fact that the object as it appears in the images is displaced and distorted relative to its actual position. Consequently, there is not a one-to-one relationship between voxels in the image and corresponding volume elements in the reference object. We used rigid registration to reduce this misregistration effect. The misregistration effect is relevant for 4D Flow MRI analysis involving image fusion

with other cardiovascular MR images such as balanced steady-state free precession (bSSFP) images of the heart or contrast-enhanced magnetic resonance angiography (CE-MRA) images of the aorta. The reference respiratory position for cardiovascular MRI is typically taken as the end-expiration and clinical images such as cardiac bSSFP or aorta CE-MRA images are typically acquired during end-expiratory breath-holds. Similarly, respiratory gating methods used with 4D Flow MRI accept data during end-expiration. However, the gating-window size is typically around 7 mm (13). Consequently, the average position of the heart or proximal aorta during a 4D Flow MRI acquisition differs by up to a few millimeters when compared with the average position of the heart or aorta during a breath-held bSSFP or CE-MRA image acquisition.

CONCLUSIONS

In conclusion, respiratory motion reduces image quality in 4D Flow MRI. The impact of the reduced image quality on flow parameters such as net flow may depend on the direction of the evaluated vessel relative to the direction of respiratory motion. Motion suppression techniques can be used to reduce the impact of motion and techniques that take into account the fact that the fidelity of the center of k-space is a major determinant for image quality appear to be more efficient than methods that treat the entire k-space in the same way. Spatial resolutions finer than the degree of accepted respiratory motion do not result in improved data quality.

ACKNOWLEDGMENTS

The authors acknowledge Jonas Lantz for providing the CFD data. The Swedish National Infrastructure for Computing (SNIC) is acknowledged for computational resources provided by the National Supercomputer Centre (Grant No. SNIC2014-11-22).

REFERENCES

1. Bailes D, Gilderdale D, Bydder G, Collins A, Firmin D. Respiratory ordered phase encoding (ROPE): a method for reducing respiratory motion artefacts in MR imaging. J Comput Assist Tomogr 1985;9:835–838.
2. Xiang QS, Henkelman RM. K-space description for MR imaging of dynamic objects. Magn Reson Med 1993;29:422–428.
3. Wang Y, Riederer SJ, Ehman RL. Respiratory motion of the heart: kinematics and the implications for the spatial resolution in coronary imaging. Magn Reson Med 1995;33:713–719.
4. Ehman RL, Felmlee JP. Adaptive technique for high-definition MR imaging of moving structures. Radiology 1989;173:255–263.
5. Larson AC, Kellman P, Arai A, Hirsch GA, McVeigh E, Li D, Simonetti OP. Preliminary investigation of respiratory self-gating for free-breathing segmented cine MRI. Magn Reson Med 2005;53:159–168.
6. Stehning C, Börnert P, Nehrke K, Eggers H, Stuber M. Free-breathing whole-heart coronary MRA with 3D radial SSFP and self-navigated image reconstruction. Magn Reson Med 2005;54:476–480.
7. Uribe S, Beerbaum P, Sørensen TS, Rasmusson A, Razavi R, Schaeffter T. Four-dimensional (4D) flow of the whole heart and great vessels using real-time respiratory self-gating. Magn Reson Med 2009;62:984–992.
8. Haacke EM, Patrick JL. Reducing motion artifacts in two-dimensional Fourier transform imaging. Magn Reson Imaging 1986;4:359–376.
9. Weiger M, Börnert P, Proksa R, Schäffter T, Haase A. Motion-adapted gating based on k-space weighting for reduction of respiratory motion artifacts. Magn Reson Med 1997;38:322–333.
10. Jhooti P, Wiesmann F, Taylor AM, Gatehouse PD, Yang GZ, Keegan J, Pennell DJ, Firmin DN. Hybrid ordered phase encoding (HOPE): an improved approach for respiratory artifact reduction. J Magn Reson Imaging 1998;8:968–980.
11. Jhooti P, Gatehouse P, Keegan J, Bunce N, Taylor A, Firmin D. Phase ordering with automatic window selection (PAWS): a novel motion-resistant technique for 3D coronary imaging. Magn Reson Med 2000;43:470–480.
12. Hackenbroch M, Nehrke K, Gieseke J, Meyer C, Tiemann K, Litt H, Dewald O, Naehle C, Schild H, Sommer T. 3D motion adapted gating (3D MAG): a new navigator technique for accelerated acquisition of free breathing navigator gated 3D coronary MR-angiography. Eur Radiol 2005;15:1598–1606.
13. Dyverfeldt P, Bissell M, Barker AJ, Bolger AF, Carlhäll C-J, Ebbers T, Francios CJ, Frydrychowicz A, Geiger J, Giese D. 4D flow cardiovascular magnetic resonance consensus statement. J Cardiovasc Magn Reson 2015;17:1–19.
14. Uribe S, Muthurangu V, Boubertakh R, Schaeffter T, Razavi R, Hill DL, Hansen MS. Whole-heart cine MRI using real-time respiratory self-gating. Magn Reson Med 2007;57:606–613.
15. Markl M, Chan FP, Alley MT, et al. Time-resolved three-dimensional phase-contrast MRI. J Magn Reson Imaging 2003;17:499–506.
16. Markl M, Harloff A, Bley TA, Zaitsev M, Jung B, Weigang E, Langer M, Hennig J, Frydrychowicz A. Time-resolved 3D MR velocity mapping at 3T: improved navigator-gated assessment of vascular anatomy and blood flow. J Magn Reson Imaging 2007;25:824–831.
17. Akçakaya M, Gulaka P, Basha TA, Ngo LH, Manning WJ, Nezafat R. Free-breathing phase contrast MRI with near 100% respiratory navigator efficiency using k-space-dependent respiratory gating. Magn Reson Med 2014;71:2172–2179.
18. van Ooij P, Semaan E, Schnell S, Giri S, Stankovic Z, Carr J, Barker AJ, Markl M. Improved respiratory navigator gating for thoracic 4D flow MRI. Magn Reson Imaging 2015;33:992–999.
19. Nordmeyer S, Riesenkampff E, Crelier G, Khasheei A, Schnackenburg B, Berger F, Kuehne T. Flow-sensitive four-dimensional cine magnetic resonance imaging for offline blood flow quantification in multiple vessels: a validation study. J Magn Reson Imaging 2010;32:677–683.
20. Valverde I, Nordmeyer S, Uribe S, Greil G, Berger F, Kuehne T, Beerbaum P. Systemic-to-pulmonary collateral flow in patients with palliated univentricular heart physiology: measurement using cardiovascular magnetic resonance 4D velocity acquisition. J Cardiovasc Magn Reson 2012;14:25.
21. Kanski M, Töger J, Steding-Ehrenborg K, Xanthis C, Bloch KM, Heiberg E, Carlsson M, Arheden H. Whole-heart four-dimensional flow can be acquired with preserved quality without respiratory gating, facilitating clinical use: a head-to-head comparison. BMC Med Imaging 2015;15:1.
22. Lantz J, Dyverfeldt P, Ebbers T. Improving blood flow simulations by incorporating measured subject-specific wall motion. Cardiovasc Eng Technol 2014;5:261–269.
23. Firmin D, Keegan J. Navigator echoes in cardiac magnetic resonance. J Cardiovasc Magn Reson 2001;3:183–193.